Received: 26 May 2021 | Revised: 6 July 2021 | Accepted: 12 July 2021

IET Systems Biology

DOI: 10.1049/syb2.12033

The Institution of Engineering and Technology WILEY

ORIGINAL RESEARCH PAPER

Multi-model fusion of classifiers for blood pressure estimation

Qi Ye | Bingo Wing-Kuen Ling | Nuo Xu | Yuxin Lin | Lingyue Hu

Information Engineering, Guangdong University of Technology, Guangzhou, China

Correspondence

Bingo Wing-Kuen Ling, Information Engineering, Guangdong University of Technology, Guangzhou, 510006, China.
Email: yongquanling@gdut.edu.cn

Funding information

Guangdong Higher Education Engineering Technology Research Centre for Big Data on Manufacturing Knowledge Patent, Grant/Award Number: 501130144; Hong Kong Innovation and Technology Commission, Enterprise Support Scheme, Grant/Award Number: S/E/070/17; National Nature Science Foundation of China, Grant/Award Numbers: U1701266, 61671163 and 62071128; Team Project of the Education Ministry of the Guangdong Province, Grant/Award Number: 2017KCXTD011

Abstract

Prehypertension is a new risky disease defined in the seventh report issued by the Joint National Commission. Hence, detecting prehypertension in time plays a very important role in protecting human lives. This study proposes a method for categorising blood pressure values into two classes, namely the class of healthy blood pressure values and the class of prehypertension blood pressure values, as well as estimating the blood pressure values continuously only by employing photoplethysmograms. First, the denoising of photoplethysmograms is performed via a discrete cosine transform approach. Then, the features of the photoplethysmograms in both the time domain and the frequency domain are extracted. Next, the feature vectors are categorised into the two classes of blood pressure values by a multi-model fusion of the classifiers. Here, the support vector machine, the random forest and the *K*-nearest neighbour classifier are employed for performing the fusion. There are two types of blood pressure values. They are the systolic blood pressure values and the diastolic blood pressure values. For each class and each type of blood pressure values, support vector regression is used to estimate the blood pressure values. Since different classes and different types of blood pressure values are considered separately, the proposed method achieves an accurate estimation. The computed numerical simulation results show that the proposed method based on the multi-model fusion of the classifiers achieves both higher classification accuracy and higher regression accuracy than the individual classification methods.

1 | INTRODUCTION

Due to the improvement in global economy, the total number of overweight and obese people is rising. This results in more incidences of cardiovascular diseases, which are the common causes of death and disabilities among humans. The guidelines issued by the American College of Cardiology/American Heart Association (ACC/AHA) define systolic blood pressure values between 120 and 129 mmHg and diastolic blood pressure values higher than 80 mmHg as the blood pressure values corresponding to elevated blood pressure [1]. In this study, systolic blood pressure values between 120 and 139 mmHg and diastolic blood pressure values between 80 and 89 mmHg were defined as the prehypertension blood pressure values. Since hypertension is a major cause for cardiovascular diseases [2], prehypertension is also defined as a new risky disease [3]. On the other hand, hypertension blood pressure values are also used as a major syndrome for performing the diagnosis of cardiovascular diseases. Hence, a continuous and accurate estimation of the blood pressure values as well as detection of prehypertension and alerting people regarding the occurrences of cardiovascular diseases play an important role in human lives.

In clinical practice, the cuff-based method or the intra-arterial cannulation-based method are usually used to estimate the blood pressure values. However, the former cannot perform continuous measurement and it is inconvenient for performing signal acquisition. On the other hand, the latter is invasive, which my put the users at risk of infection. Therefore, there is a need for a non-invasive and continuous blood

pressure monitoring system. The continuous estimation of blood pressure values via wearable and non-invasive signal acquisition methods has recently been developed. Here, both electrocardiograms and photoplethysmograms are employed for performing the estimation [4]. However, it is worth noting that electrocardiograms detect electrical signals. The quality of electrocardiograms is degraded in the presence jewellery or metallic objects in the body during the signal acquisition process. Nevertheless, it is not easy to remove metallic objects such as dental implants. Moreover, the major feature extracted from electrocardiograms and photoplethysmograms used for estimating the blood pressure values is the pulse transit time. However, extracting this feature requires synchronisation between the electrocardiograms and the photoplethysmograms, which causes difficulty in designing and implementing the hardware device. On the other hand, photoplethysmograms are optically obtained plethysmograms. They are versatile and easier to be acquired [5]. The estimation of blood pressure values by employing only photoplethysmograms became more realistic with the emergence of digital sensors [6]. Therefore, this study only employs photoplethysmograms for continuously estimating the blood pressure values.

It is worth noting that the relationship between photoplethysmograms and blood pressure values is unknown. Hence, the machine learning approach is employed to build the model. The common machine learning methods include the support vector machine, the random forest and the *K*-nearest neighbour classifier. However, different machine learning methods have their strengths and weaknesses. Hence, this study proposes a fusion approach to integrate different machine learning methods to perform blood pressure estimation. The rest of this study is as follows: Section 2 presents the denoising method for improving the quality of the acquired photoplethysmograms. Section 3 presents the method for performing feature extraction. Section 4 reviews three popular classification models. Section 5 presents a multi-model fusion of the classifiers. Section 6 presents the computed numerical simulation results. Finally, a conclusion is drawn in Section 7.

2 | DENOISING OF PHOTOPLETHYSMOGRAMS

This study proposes a discrete cosine transform-based method for performing the denoising of photoplethysmograms. Here, the proposed method consists of two approaches. One is to perform lowpass filtering by only selecting the coefficients in the lowpass frequency band. Another approach is to perform thresholding by only selecting the large magnitude coefficients. The details are discussed below.

2.1 | Dataset

There are 219 subjects from the Guilin People's Hospital in the Guang-Xi Province of China. They consented prior to the study via written letters. As many photoplethysmograms are of poor quality, they cannot be used for extracting the features. Therefore, only 246 photoplethysmograms are retained. Here, 104 photoplethysmograms are from healthy subjects with normal blood pressure values and 142 photoplethysmograms are from subjects with prehypertension blood pressure values. As a wide range of the blood pressure values is covered, this dataset is highly representative.

In this study, the photoplethysmograms are sampled at 1000 Hz. Hence, a photoplethysmogram with 2100 points contains more than one pulse. Therefore, the photoplethysmograms are segmented into pieces, with each piece containing 2100 points. Besides, the corresponding invasive blood pressure values are used as the reference values for performing the training.

2.2 | Denoising algorithm

In this study, the discrete cosine transform [7] is used to perform the denoising of the photoplethysmograms. For each photoplethysmogram, the following procedures are performed:

Step 0 Denote the threshold value as E.

Step 1 The discrete cosine transform coefficients of the photoplethysmogram are computed.

Step 2a The absolute values of the entire discrete cosine transform alternating current coefficients are sorted in descending order.

Step 2b The first 32 largest discrete cosine transform alternating current coefficients are selected and the remaining discrete cosine transform alternating current coefficients are set to zero.

Step 2c First, initialise a zero vector. In each iteration, a discrete cosine transform alternating current coefficient is selected starting from the maximum absolute value of these 32 coefficients. The corresponding zero in the initialised vector is replaced by this selected coefficient. This step is repeated until the ratio of the sum of the energy of the selected discrete cosine transform alternating current coefficients to the sum of the energy of all these 32 discrete cosine transform alternating current coefficients reaches the value of E. Then, the first zero in the initialised vector is replaced by the discrete cosine transform direct current coefficient. Next, the inverse discrete cosine transform is applied to this initialised vector to obtain the denoised photoplethysmogram.

Step 3 Find the maximum point of the denoised photoplethysmogram. Then, construct a local neighbourhood around this maximum point. where there are 249 points and 450 points on the left and on the right side

of this maximum point, respectively. Here, this local neighbourhood of the photoplethysmogram contains 700 points and should include a single pulse of the photoplethysmogram.

Step 4 This first order derivative of the photoplethysmogram is called the velocity of the photoplethysmogram. The velocity of the photoplethysmogram within this local neighbourhood is computed. If the total number of the peaks of the velocity of the photoplethysmogram within this local neighbourhood is more than the threshold number denoted as Q, then E is reduced by a ratio denoted as R and we go back to Step 2c.

Step 5 The obtained signal is taken as the final denoised photoplethysmogram for performing the feature extraction discussed in the next section.

The working principle of the proposed denoising algorithm is as follows: Since the photoplethysmograms are oversampled, the clean photoplethysmograms are the narrow band signals and the noises are the wide band signals. As a result, the signal-to-noise ratio of the photoplethysmograms can be improved if only the first several discrete cosine transform coefficients are retained. In particular, since the heart rate of majority of the people is less than 115 pulses per minute and the sampling rate of the photoplethysmograms is 1000 Hz, the maximum frequencies of the photoplethysmograms are located before the $((115 \times 2100)/(60 \times 1000))^{th}$ discrete cosine transform coefficient. However, as the photoplethysmograms contain around 8 harmonics of the fundamental frequencies, $((115 \times 2100 \times 8)/(60 \times 1000)) \approx 32$ discrete cosine transform coefficients are retained. Besides, the clean photoplethysmograms have large magnitudes in the passbands, while the noises have low magnitudes in the whole frequency band and the signal-to-noise ratios of photoplethysmograms can be increased by setting the discrete cosine transform coefficients with the small values to zero. Moreover, if the noises are detected, then the noises should be further suppressed by reconstructing the signal using a smaller number of the discrete cosine transform coefficients. Hence, the above procedures are repeated by using a smaller value of E, if the noises are detected.

It is worth noting that only 32 discrete cosine transform coefficients are picked up in Step 2b. Hence, the photoplethysmograms basically occupy the whole frequency band defined by these 32 discrete cosine transform coefficients. As a result, most of the discrete cosine transform coefficients should be selected and E should be initialised to a value close to 1. Therefore, this study chooses the value of E as 0.999. Likewise, R should be small to guarantee that only a very small number of the discrete cosine transform coefficients is discarded in the next iteration. Therefore, this study chooses the value of R as 0.001. On the other hand, an ideal photoplethysmogram is shown in Figure 2. It can be seen that a pulse of the photoplethysmogram consists of two durations, with each duration starting with the positive slope. This implies that the total number of the peaks in the first order derivative of the photoplethysmogram within a pulse is equal to 2. Hence, the noise can be detected in the time domain if the total number of the peaks in the first order derivative of the photoplethysmogram within a pulse is greater than 3. Therefore, this study chooses the value of Q as 3.

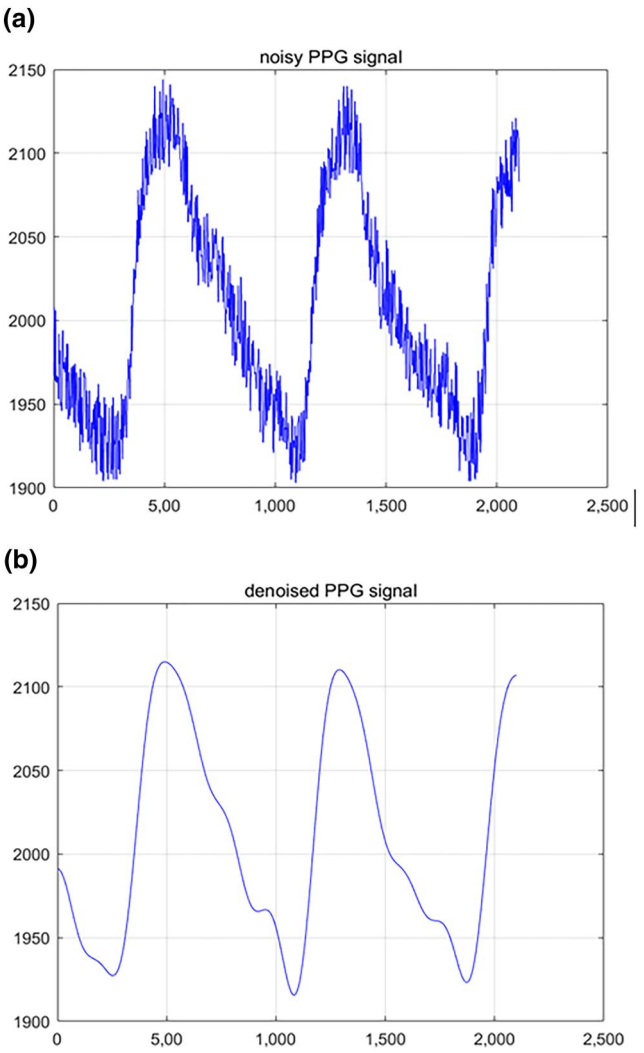

FIGURE 1 (a) A noisy photoplethysmogram. (b) The corresponding denoised photoplethysmogram

Figure 1 shows a realisation of the noisy photoplethysmogram and the corresponding denoised photoplethysmogram. It can be seen from Figure 1 that the noise is significantly reduced. This demonstrates the effectiveness of the proposed denoising algorithm.

3 | FEATURE EXTRACTION

In this study, the features of the photoplethysmograms in both the time domain and the frequency domain are extracted.

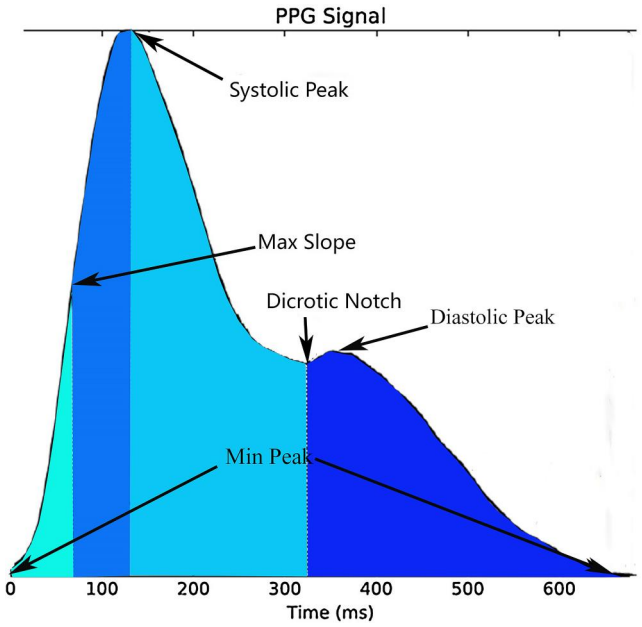

FIGURE 2 The points in the photoplethysmogram for extracting the features in the time domain

3.1 | Features in the time domain

Figure 2 shows the points in an ideal photoplethysmogram for extracting the features in the time domain. In particular, they include the following:

1. The time interval between the systolic peak and the dicrotic notch
2. The ratio of the systolic peak to the dicrotic notch
3. The ratio of the systolic peak to the diastolic peak
4. The area under the photoplethysmogram within the time interval between the minimum peak and the maximum slope
5. The area under the photoplethysmogram within the time interval between the maximum slope and the systolic peak
6. The area under the photoplethysmogram within the time interval between the systolic peak and the dicrotic notch
7. The area under the photoplethysmogram within the time interval between the dicrotic notch and the minimum peak
8. The total number of heart beats per minute.

Further details of these time domain features can be found in [8].

3.2 | Features in the frequency domain

The discrete cosine transform coefficients of the photoplethysmograms are computed. Since around 20 discrete cosine transform coefficients are selected in the denoising algorithm, only 20 discrete cosine transform coefficients are employed as features in the frequency domain for estimating the blood pressure values [9].

3.3 | Feature selection

By using the random forest to rank the importance of the features [10], four features are removed. In particular, the second feature and the fifth feature in the time domain and the fifth feature and the sixth feature in the frequency domain are removed. As a result, 24 features are extracted from each photoplethysmogram and they form a feature vector for estimating the blood pressure values.

4 | REVIEWS ON THE EXISTING CLASSIFICATION MODELS

In this study, the support vector machine, the random forest and the K-nearest neighbour classifier are employed for performing the fusion of the classifiers.

4.1 | Support vector machine

The support vector machine is a two-class classifier. It consists of a non-linear kernel and a conventional perceptron. Here, the perceptron is designed based on maximising the minimum distance between two manifolds, with each manifold representing an individual class of objects. In fact, finding the hyperplane for dividing these two manifolds with the largest geometric margin is an H_∞ optimisation problem. For more details about the support vector machine, please refer to [11].

Let N and n be the total number and the dimension of the feature vectors, respectively. Let $x_i \in R^n$ be these feature vectors. Let y_i be the corresponding classes of the objects. Here, these two classes of the objects are represented by $+1$ and -1. Then, $y_i \in \{+1, -1\}$. When $y_i = +1$, x_i belongs to a positive class of the objects. When $y_i = -1$, x_i belongs to a negative class of the objects. Let T be the set of the input output pairs. That is,

$$T = \{(x_1, y_1), (x_2, y_2), \ldots, (x_N, y_N)\} \tag{1}$$

Let $f(\cdot)$ be the kernel function and w be the vector representing the hyperplane for separating these two manifolds. Then, the design of the hyperplane is formulated as the following optimisation problem:

$$\max_{w} \quad \varepsilon, \tag{2a}$$

subject to

$$y_i f^T(x_i) w \geq \varepsilon \quad \text{for } i = 1, \cdots, N, \tag{2b}$$

and

$$\varepsilon \geq 0^+. \tag{2c}$$

This optimisation problem can be re-cast to a linear programing problem and many efficient algorithms such as the

simplex method can be employed for finding the solution of this optimisation problem.

4.2 | Random forest

The random forest is an ensemble-based bagging algorithm. In particular, the random forest selects the feature vectors randomly for generating the decision trees. Let M be the total number of the feature vectors to be extracted from the original training set by the bootstrap method [12]. Let L be the total number of the features to be randomly selected from all the features. The best partitioning feature is selected as the node to construct a decision tree. Each decision tree is a weak learner. The class with the most votes from all the weak learners is taken as the final classification output [13].

It is worth noting that a feature is selected among all the features and a node divides the decision tree into the left subtree and the right subtree in conventional decision tree-based methods [14]. Compared to the conventional decision tree-based methods, the random forest improves the formation of the decision trees in the following senses: The random forest randomly selects some features from all of the features. Then, an optimal feature is selected from among these randomly selected features to partition the decision tree into the left subtree and the right subtree. This further enhances the generalisation ability of the model.

4.3 | K-nearest neighbour classifier

The K-nearest neighbour classifier makes a classification decision based on the K-nearest neighbours around a particular point. Here, the value of K, the distance measured and the decision rule for determining the class are the three basic elements of the K-nearest neighbour algorithm [15]. When these three elements are pre-defined, the classification of an input feature vector partitions the feature space into subspaces, with each subspace representing a class of objects.

5 | MULTI-MODEL FUSION OF THE CLASSIFIERS

This study classifies these 246 photoplethysmograms into two classes of blood pressure values, namely the healthy class of the blood pressure values and the prehypertension class of the blood pressure values. It is worth noting that there are other classes of blood pressure values as well. However, the total number of samples for the other classes of blood pressure values is very small. Hence, this study ignores these small classes of blood pressure values. Besides, it is worth noting that there are two types of blood pressure values. They are the systolic blood pressure values and the diastolic blood pressure values.

Since the blood pressure varies as the body activity varies, there is an overlap between the range of the healthy blood pressure values and that of the prehypertension blood pressure values. Hence, in order to classify whether the acquired photoplethysmograms belong to the healthy blood pressure values or the prehypertension blood pressure values, the reference blood pressure values are not used for performing this classification. Instead, the reference blood pressure classes defined by the medical experts are employed.

For each type of the blood pressure values, all the feature vectors are randomly divided into training set A and test set B without the overlap. Here, training set A and test set B contain 80% and 20% of all the feature vectors, respectively. Training set A is further divided into training set C and training set D without the overlap. Here, the ratio of the total number of the feature vectors in training set C to that in training set D is 1:3. The detailed procedures for performing the multi-model fusion of the classifiers are as follows:

Step 1 The input–output pairs in training set C is used to train the classification models based on the random forest, the K-nearest neighbour classifier and the support vector machine.

Step 2 The input–output pairs in training set D is used to verify these three classification models obtained in Step 1. First, the predicted classes of the blood pressure values are obtained. Then, symbol '1' is notated if the predicted class is the same as the actual class. Otherwise, symbol '0' is notated if the predicted class is different from the actual class. Now, there are eight possibilities representing the classification accuracies of these three classifiers for each feature vector in training set D. Table 1 shows these eight possibilities.

Step 3 The feature vectors in training set D and their corresponding identity numbers representing the possibilities of the accuracies of the classifiers defined in Table 1 are used to train an accuracy model based on the random forest.

TABLE 1 The eight possibilities of the accuracies of the classifiers based on the feature vectors in training set D

Random forest	Support vector machine	*K*-nearest neighbour	Identity number representing the possibilities
1	1	1	7
1	1	0	6
1	0	1	5
1	0	0	4
0	1	1	3
0	1	0	2
0	0	1	1
0	0	0	0

Step 4 The feature vectors in test set B are used to predict the classes of the blood pressure values using the three classification models obtained in Step 1. Moreover, the feature vectors in test set B are also used to predict the accuracy of various classifiers using the accuracy model obtained in Step 3. Since the symbol representing 1 refers to the class predicted by the corresponding classifier being the same as the actual class for this feature vector, the class predicted by the corresponding classifier remains changed. On the other hand, since the symbol representing 0 refers to the class predicted by the corresponding classifier being different from the actual class for this feature vector, the class predicted by the corresponding classifier is changed to another class. Then, the final class of the blood pressure values is determined based on the majority votes among these three processed predicted classes of the blood pressure values.

Finally, the blood pressure values are estimated as follows: For each group and each type of the blood pressure values, the feature vectors and the corresponding blood pressure values in training set A are used to train the regression model via the support vector regression. Then, the feature vectors in test set B are used to verify the support vector regression models.

6 | COMPUTED NUMERICAL SIMULATION RESULTS

In this study, the average accuracy and the average root mean square error are employed as the metrics of classification and regression, respectively, for evaluating the performance of various methods. In order to obtain the more reliable results, the cross-validation approach is employed, that is, the dataset used for performing the classification and the regression is randomly shuffled 50 times. Then, various methods are applied for the shuffled data. Finally, the average root mean square error and the average accuracy are computed for evaluating the performances of various methods.

Since the proposed method is based on a fusion of three individual classification methods, it is meaningful to compare the individual classification methods to verify whether the fusion algorithm is effective or not. Table 2 shows the average classification accuracies obtained based on these three individual classification models and the proposed fusion method. Further, Table 3 shows the root mean square errors obtained based on these three individual classification models and the proposed fusion method. As the proposed method has considered the classification accuracies of the individual models and the decision is performed based on majority vote, the obtained result is more reliable. Besides, as the accuracies of the individual models have been considered and the incorrect classification results have been corrected based on the photoplethysmograms, the proposed method can further improve the overall classification accuracy based on the photoplethysmograms. This improvement is reflected by the results shown in Table 2 and Table 3. The accuracy achieved by the proposed fusion method is higher than that achieved by the individual classification models. Also, the root mean square errors achieved by the proposed fusion method are lower than those achieved by the individual classification models. This concludes that the proposed fusion method outperforms the individual classification models.

In order to test the robustness of the proposed method, the ratio of the total number of the feature vectors in training set A to that in test set B is changed to 9:1. Training set A is further divided into training set C and training set D without the overlap. Here, the ratio of the total number of feature vectors in training set C to that in training set D is 2:7. The average accuracy and the average root mean square error are shown in Table 4 and Table 5, respectively. It can be seen that similar results are obtained. Hence, the proposed method is robust.

To evaluate the required computational complexity of the proposed algorithm, the total time taken for these three single classification algorithms and the proposed algorithm are listed in Table 6. Although the proposed method takes longer time than the single classification methods, the total time taken

TABLE 2 The classification accuracies obtained based on these three individual classification models and the proposed fusion method

Random forest	Support vector machine	*K*-nearest neighbour	The proposed method
67.2653%	51.9592%	61.5510%	72.3265%

TABLE 3 The root mean square errors obtained based on these three individual classification models and the proposed fusion method

	Random forest	Support vector machine	*K*-nearest neighbour	The proposed method
Systolic blood pressure	11.2854	14.6151	11.8264	10.8386
Diastolic blood pressure	7.7366	8.5006	8.1031	7.6445

TABLE 4 The classification accuracies obtained based on these three individual classification models and the proposed fusion method

Random forest	Support vector machine	*K*-nearest neighbour	The proposed method
68.4800%	51.3600%	65.6800%	73.2000%

TABLE 5 The root mean square errors obtained based on these three individual classification models and the proposed fusion method

	Random forest	Support vector machine	*K*-nearest neighbour	The proposed method
Systolic blood pressure	10.9843	14.8042	11.3881	10.3430
Diastolic blood pressure	7.4139	8.1946	7.4996	6.9961

TABLE 6 The total time taken for these three individual classification models and the proposed fusion method

Random forest	Support vector machine	*K*-nearest neighbour	The proposed method
0.25 s	0.0075 s	0.010 s	0.66 s

based on the proposed method is less than 1 s, which is acceptable for the majority of consumer electronics-based applications.

7 | CONCLUSION

This study proposes a multi-model fusion of classifiers for estimating blood pressure values. Here, only photoplethysmograms are acquired via a wearable and non-invasive device. First, the discrete cosine transform approach is employed for performing the denoising of the photoplethysmograms. There are two types of blood pressure values. They are the systolic blood pressure values and the diastolic blood pressure values. Further, there are two classes of blood pressure values. They are the healthy blood pressure values and the prehypertension blood pressure values. First, a part of the training data is used to train three different classifiers for performing the classification of the blood pressure values. Another part of the training data is used for verifying the classification of the blood pressure values. The obtained results are used to train a model based on the accuracy of various classifiers. For the test data, these three classifiers are used for performing the classification of the blood pressure values. Also, the model based on the accuracy of various classifiers is used to modify the classes predicted by the individual classifiers. The final class of blood pressure values is determined based on majority votes among these three modified predicted classes of blood pressure values. Finally, support vector regression is used to estimate the blood pressure values for each type and each class of blood pressure values. The computed numerical simulation results show that the proposed method achieves higher classification accuracy and lower mean square errors than the individual classification models.

Since the proposed method is based on a supervised learning approach, one of the limitations of the proposed method is that a strong correlation between the training data and the test data is required. In future, the physical mechanism governing the relationship between the blood pressure values and the reflection intensity of infrared light will be investigated. The obtained results will be compared with those obtained by the ambulatory blood pressure monitoring system. Besides, the blood glucose monitoring function will be developed via the wearable non-invasive device because it cannot be developed via the ambulatory blood pressure monitoring system.

ACKNOWLEDGMENTS

This study was supported partly by the National Nature Science Foundation of China (no. U1701266, no. 61,671,163 and no. 62,071,128), the Team Project of the Education Ministry of the Guangdong Province (no. 2017KCXTD011), the Guangdong Higher Education Engineering Technology Research Centre for Big Data on Manufacturing Knowledge Patent (no. 501,130,144) and the Hong Kong Innovation and Technology Commission, Enterprise Support Scheme (no. S/E/070/17).

ORCID

Bingo Wing-Kuen Ling https://orcid.org/0000-0002-0633-7224

REFERENCES

1. Whelton, P.K., et al.: ACC/AHA/AAPA/ABC/ACPM/AGS/APhA/ASH/ASPC/NMA/PCNA guideline for the prevention, detection, evaluation, and management of high blood pressure in adults: a report of the American College of Cardiology/American Heart Association Task Force on Clinical Practice Guidelines. JACC (J Am. Coll. Cardiol.) 71, e127–e248 (2017)
2. Lim, S.S., et al.: A comparative risk assessment of burden of disease and injury attributable to 67 risk factors and risk factor clusters in 21 regions 1990–2010: a systematic analysis for the global burden of disease study 2010. Lancet. 380, 2224–2260 (2013)
3. Heather, A., et al.: Prehypertension and cardiovascular morbidity. Ann. Fam. Med. 3, 294–299 (2005)
4. Douniama, C., Sauter, C.U., Couronne, R.: Blood pressure tracking capabilities of pulse transit times in different arterial segments: a clinical evaluation. In: IEEE Computers in Cardiology Conference, 201–204 (2009)
5. Elgendi, M.: On the analysis of fingertip photoplethysmogram signals. Curr. Cardiol. Rev. 8, 14–25 (2012)
6. Liang, Y., et al.: Photoplethysmography and deep learning: enhancing hypertension risk stratification. Biosensors. 8, 101 (2018)
7. Ahmed, N., Natarajan, T., Rao, K.R.: Discrete cosine transform. IEEE Trans. Comput. 100, 90–93 (1974)
8. Mohebbian, M.R., et al.: Blind, cuff-less, calibration-free and continuous blood pressure estimation using optimised inductive group method of data handling. Biomed. Signal Process Contr. 57, 101682 (2020)
9. Wang, Z., Zhang, Y.: A novel frequency domain method for estihemating blood pressure from photoplethysmogram. In: Proceedings of the 9th International Conference on Signal Processing Systems, 201–206 (2017)
10. Menze, B.H., et al.: A comparison of random forest and its Gini importance with standard chemometric methods for the feature selection and classification of spectral data. BMC Bioinf. 10, 213 (2009)
11. Burges, C.J.C.: A tutorial on support vector machines for pattern recognition. Data. Min. Knowl. Discov. 2, 121–167 (1998)
12. Horowitz, J.L.: The bootstrap. Handb. Econom. 5, 3159–3228 (2001)

13. Liaw, A., Wiener, M.: Classification and regression by random forest. R. News. 2, 18–22 (2002)
14. Jin, C., Luo, D.L., Mu, F.X.: An improved ID3 decision tree algorithm. In: The 4th IEEE International Conference on Computer Science and Education. 127, 130 (2009)
15. Peterson, L.E.: K-nearest neighbour. Scholarpedia. 4, 1883 (2009)

How to cite this article: Ye, Q., et al.: Multi-model fusion of classifiers for blood pressure estimation. IET Syst. Biol. 15(6), 184–191 (2021). https://doi.org/10.1049/syb2.12033